J. Plasma Physics (2006), *vol.* 72, *part* 6, *pp.* 791–794.
doi:10.1017/S0022377806004892 Printed in the United Kingdom

The formation of high-density core plasma in non-spherical implosion using high-resolution two-dimensional integrated implosion code

H. NAGATOMO[1], T. JOHZAKI[1], A. SUNAHARA[2] and K. MIMA[1]

[1]Institute of Laser Engineering, Osaka University, 2-6 Yamadaoka Suita, Osaka 565-0871, Japan

[2]Institute for Laser Technology, 2-6 Yamadaoka Suita, Osaka 565-0871, Japan

(Received 18 August 2005 and accepted 9 December 2005)

Abstract. Fast ignition is an epoch-making scheme for inertial fusion energy. In this scheme, the formation of high-density core plasma is one of the key issues which must be solved, because the implosion dynamics of the fast ignition target, which is non-spherical with a conical target, is quite different from that of the conventional central ignition target. Some previous works showed the possibility of formation of a high-density core. However, the effects of hydrodynamic instability were not discussed in those works. In this paper, we simulate the whole implosion dynamics of a perturbed non-spherical target, and the effect of radiation transport instability is estimated using the two-dimensional integrated implosion (radiation hydrodynamics) code PINOCO. In the result, we have found that the hydrodynamic instabily has less of an effect on the formation of high-density core plasma in the cone-guided implosion, in comparision with the spherical implosion.

1. Introduction

The fast ignition scheme is one of the most fascinating and feasible ignition schemes for inertial fusion energy [1, 2]. Numerical simulation plays an important role in demonstrating the performance of fast ignition, designing the targets and optimizing laser pulse shapes for the scheme. One of the key issues in fast ignition is controlling the implosion dynamics to form high-density core plasma in non-spherical implosion. Some previous works showed the possibility of formation of a high-density core plasma [3]. However, in those simulations, the non-uniformity of the initial target or laser irradiation are not included, and the effects of hydrodynamic instability were not discussed. Therefore, preliminary simulations are performed to demonstrate the effect of radiation transport (RT) instability, which is seeded by the perturbation on the initial target surface. It may be difficult to simulate the problem with a conventional Lagrangian-based implosion code for the rezoning/remapping problem. Here, a two-dimensional integrated implosion code, PINOCO, is applied for the simulations. In this code, almost all of the physics models which are required to simulate the laser-driven implosion are included. In this paper, an outline of PINOCO is given briefly, and we discuss the simulated results of cone-guided implosion with/without initial perturbation on the target surface.

2. Numerical methods

In PINOCO, mass, momentum, electron energy, ion energy, equation of states, laser ray-trace, laser absorption, radiation transport, surface tracing and other related equations are solved simultaneously [3, 4]. In most of the integrated implosion codes except PINOCO, hydrodynamic equations are solved by Lagragian-based arbitrary Lagrangian Eulerian (ALE) methods. However, they are easily affected by numerical viscosity at the rezoning/remapping process. Therefore, we have extended CIP (Constrained Interpdation profile) method [5] into an ALE type CIP method, the so-called ALE–CIP. This modification has enabled the calculation of a large dynamic range of the implosion. Originally, CIP has some of the characteristics of a Lagrangian method, although the fundamental formulas are for Eulerian coordinates. This CIP method is also employed to track the interface between the different materials clearly. This tracking system is very useful when multi-material target structures must be considered. The equation of state is based on quotidian equation of state (QEOS) [6] with a fitting formula [7].

In the energy equations, a flux-limited Spitzer–Harm-type thermal transport model is solved using the implicit nine-point differencing of the diffusion equation with ICCG (Incomplete Cholesky, Conjugate Gradient) method. For the laser ray-trace, a simple one-dimensional ray-tracing method is applied. The RT solver is newly installed. Here, multi-group flux-limited diffusion-type equations are solved with the ILUBCG (Incomplete LU Biconjugate Gradient) implicit method. In the calculation of opacity and emissivity, LTE (Local Thermal Equilibrium) and CRE (Collisional Radiative Equilibrium) models are prepared for table lookup.

Even though we can move the grid points in a Lagrangian way in PINOCO simulation, the so-called sliding mesh, in which the high-resolution region is sliding along the mass center of the target, is used in all of these simulations. We have to remark that the advantage of the sliding mesh is not only a simple rezoning rule but also better convergence of the iteration method in solving the diffusion equations. Only an implosion code which is based on a high-order scheme such as PINOCO can simulate the whole process of the implosion with the sliding-mesh.

3. Computational results

The cone with an opening angle of 30° is attached to a spherical shell of polystyrene ($\rho = 1.06\,\mathrm{g\,cm^{-3}}$) which has a uniform thickness of 8 µm. The target is irradiated by a uniform laser, the wavelength, energy and pulse width of which are $\lambda = 0.53\,\mu\mathrm{m}$, 6.0 kJ and 1.2 ns (Gaussian, full width at half maximum), respectively. Due to the limitation of computational resources, RT is ignored in these simulations. The configuration of the target is shown in Fig. 1. The number of computational grid points is 300 ×300, these are distributed mainly in the shell target and gold cone region.

For the comparison, spherical implosions without cone targets are also simulated with the initial perturbation of mode numbers $\ell = 12$ and 24 and without perturbation. The amplitudes of the perturbation are 0.02 and 0.04 µm for the mode numbers $\ell = 12$ and 24, respectively. Figure 2 shows the density contours and ion temperature of the spherical implosion and cone-guided implosion of perturbation mode number $\ell = 24$ at $t = 1.5$ ns. Although similar dynamics are observed at the right-hand side of the shells in both cases, the dynamics of the opposite side are quite different. The surface of the gold cone is ablated and laser energy is absorbed by the ablated gold plasma in the cone-guided implosion case. In the spherical

https://doi.org/10.1017/S0022377806004892 Published online by Cambridge University Press

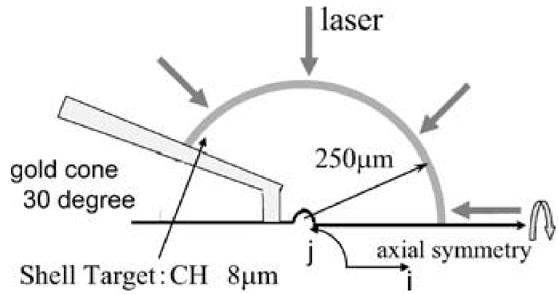

Figure 1. The cone-guided target and computational conditions.

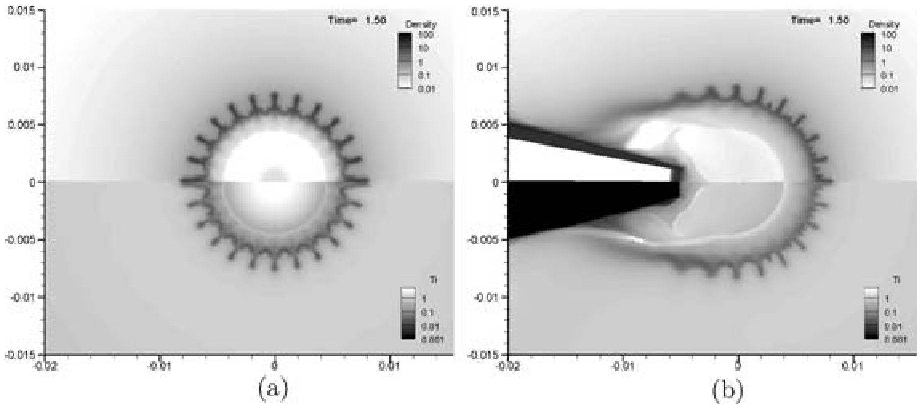

Figure 2. Density contours (above, in g cm^{-3}) and ion temperature contours (below, in KeV) at time = 1.5 ns of (a) a spherical implosion and (b) a cone-guided implosion.

implosion case, there is a hot spot where high ion temperature and high pressure appeared. In the cone-guided implosion case, the hot spot did not appear at the center of the imploson and this enabled the high-density core plasma to form. Even though there is a single mode perturbation on the surface in the cone-guided implosion case, there is another perturbation of mode 1 because of the existence of the cone. Therefore, the growth of the RT instability is much more complicated with the multi-mode RT instability, which causes the higher mode perturbations.

The ρR of the core plasma is the essential for fast ignition. Figure 3(a) shows the areal density ρR which is averaged by angle. In the figure, the spherical implosion case is also plotted. In our previous work, the ρR of the core plasma of non-spherical implosion case is higher than that of spherical implosion case. This difference is due to the strength of the first shock which destroys the tip of the cone. The input laser energy was 2.5 kJ in the previous simulation, and it is 6.0 kJ here. This means that we have to design the pulse shape carefully to reduce the impact of the first shock on the tip of the cone. The reduction ratio, which is the averaged areal density normalized by that of unperturbed case ($\rho R/\rho R_{\mathrm{mode}\,0}$), is plotted in Fig. 3(b). In the spherical implosion case, the mode number increases and the lower areal density is observed. On the other hand, it has less influence on the mode number. That is, non-spehrical implosions are robust under the nonlinear hydrodynamic instabilities.

In these simulations, the hydrodynamic instabilities of higher harmonic mode appear and grow rapidly, and they must affect the results. Even though the analysis of the higher mode instability is important, we need much finer computational grids

https://doi.org/10.1017/S0022377806004892 Published online by Cambridge University Press

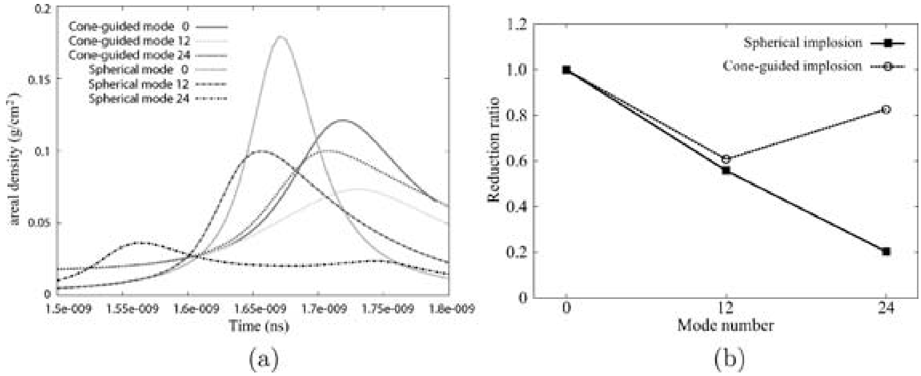

Figure 3. (a) Avereged areal density (ρR) and initial perturbation mode number. (b) Reduction ratio of the areal density ($=\rho R/\rho R_{\text{mode}\,0}$).

if we are to consider short wavelength perturbations. Also, the RT is not included in this work to save the time required for computation. It may stabilize the RT instability, and the dynamics of the gold cone will be affected by radiative heating. Research of these details will form the basis of our future work.

4. Conclusions

Preliminary simulations have been performed to study the effect of the hydrodynamics instability on the formation of a high-density core in a non-spherical implosion for the fast ignition scheme. In the results, we have found that the hydrodynamic instabily has less of an effect on the formation of high-density core plasma in the cone-guided implosion, in comparision with the spherical implosion.

In these simulations, we have ignored the RT, which is very important in the physics of the implosion, and it should be considered in the next stage.

Acknowledgements

This work was supported by a MEXT Grant-in Aid for Creative Scientific Research (15GS0214). This simulation was executed on the computers at ILE and the Cyber Media Center, Osaka University.

References

[1] Tabak, M. *et al.* 1994 Ignition and high gain with ultrapowerful lasers, *Phys. Plasmas* **1**, 1626–1634.

[2] Izawa, Y. *et al.* 2004 Petawatt Laser System for Fast Ignitor Studies at ILE, Osaka University, *Proceedings of 20th International Atomic Energy Agency*, Fusion Energy Conference, IAEA-CN-116/OV/3-2 IAEA.

[3] Nagatomo, H. *et al.* 2004 Development of Fast Ignition Integrated Interconnecting Code (FI^3) for Fast Ignition Scheme, *Proceedings of 20th International Atomic Energy Agency*, Fusion Energy Conference, IAEA-CN-116/IFP/07-29 IAEA.

[4] Nagatomo, H. *et al.* 2001 Analysis of Hydrodynamic Instabilities in Implosion using High-accuracy Integrated Implosion Code, *Proceedings of 2nd Int. Conf. on IFSA'01.*

[5] Yabe, T., Xiao, F. and Utsumi, T. 2001 The Constrained Interpolation Profile Method for Multiphase Analysis, *J. Comp. Phys.* **169**, 556–593.

[6] More, R. M. *et al.*, 1988 A new quotidian equation of state (QEOS) for hot dense matter, *Phys. Fluids* **31**(10), 3059–3078.

[7] Takami, K. and Takabe, H. 1990 Simple Fitting Formulas of Equation of State for Laser Produced Plasmas, *Tech. Rep of Osaka Univ.* **40**, No. 2005 159–173, Osaka Univ.